Environ. Sci. Technol. **2000**, *34,* 2393−2400

Magnetic Properties of Daily Sampled Total Suspended Particulates in Shanghai

JIONG SHU,*,† JOHN A. DEARING,‡ ANDREW P. MORSE,‡ LIZHONG YU,† AND CHAOYI LI†

Department of Geography, East China Normal University, Shanghai 200062, China, and Department of Geography, University of Liverpool, P.O. Box 147, Liverpool L69 7ZT, U.K.

Samples of total suspended particulates (TSPs) and <10 μm fractions (PM_{10}) collected daily from in and around two industrial districts in Shanghai, China, during November 1998 have been examined using environmental magnetic measurements. Statistical classifications of the data show that the 11 sampling sites can be classified into four categories of magnetic properties, each expressing a different combination of mainly local dust sources. Changes in meteorological conditions, particularly wind direction, cause daily shifts in particulate types and sources. Interpretation of the magnetic parameters suggests roughly constant proportions of high coercivity ("hematite") and low coercivity ("magnetite") mineral phases with a predominance of ferrimagnetic grains in superparamagnetic (SP) and multidomain (MD) + pseudo single domain (PSD) sizes. Negative linear correlations between TSP concentrations and ferrimagnetic concentration parameters suggest that the dominant source of TSPs is weakly magnetic. Mass specific susceptibility (χ_{LF}), saturation isothermal remanence (SIRM), susceptibility of anhysteretic remanent magnetization (χ_{ARM}), and high field remanence magnetization (HIRM) appear to discriminate the different dusts from a range of sources, including iron and steel manufacturing, coal-fired combustion, construction industries and wind-blown soil. Measurements on samples from modern chimney stacks suggest that magnetic phases from coal-fired combustion processes are dominantly carried in <10 μm particle fractions. Strongly ferrimagnetic particles in TSPs are probably linked more to combustion products from older technologies. PM_{10} samples appear to originate from a wide range of sources including combustion products and construction materials. Given previously reported links between magnetic properties and mutagenicity in respirable particulates, the results may help to identify areas of high health risk. The results demonstrate that magnetic measurements provide an exceptionally simple and effective approach for identifying daily variations in particulate loadings and sources in this urban environment.

Introduction

TSPs and PM_{10}s are significant hazards for health in many urban areas worldwide. Sources of particulates include those produced during high-temperature combustion of fossil fuels, metalliferous emissions, vehicle emissions, and wind-blown soil (*1*). Application of environmental magnetic techniques (*2, 3*) has now been used to study atmospheric particulates at diverse geographic locations in samples of modern suspended dusts (*4*−*8*), road dusts (*9*−*11*), polluted organic soils (*12*−*14*), contaminated building surfaces (*15*), polluted leaf and tree bark surfaces (*16*−*18*), and pre- and postindustrial sediment records (*19, 20*). The presence of Fe in virtually all these dust types, existing in a variety of chemical and physical forms, provides a basis for characterizing and monitoring dusts using easily and nondestructively measured magnetic properties. Chester et al. (*4*) distinguished two sources of soil-sized particles from the Mediterranean atmosphere by magnetic susceptibility (χ) values and showed the importance of particles derived from combustion processes. Oldfield et al. (*8*) used several concentration-independent magnetic parameters to characterize dusts from different source types. They inferred that magnetic parameters are sensitive to differences between dust arising from fossil-fuel combustion and from other industrial processes and those derived from soil erosion. Oxidation of iron sulfides in coal provides the mechanism for high-temperature production of nonstoichiometric "magnetite"-like and "hematite"-like phases in fly ash, which may be detected microscopically as magnetic spherules or through grain-size dependent magnetic parameters (*21, 22*). Flanders (*16, 17*) found a reduction in the coercive force of particulates as distance from power station point sources increased, explained by the reduced amount of fly ash relative to wind-blown soil (cf. ref *23*). Xie et al. (*10, 11, 23*), following early workers (*9*), showed that by using a wider range of magnetic measurements an interpretation in terms of magnetite grain-size may be extended to nonmagnetite minerals, such as canted antiferromagnetic hematite. Magnetic data sets are amenable to analysis by multivariate techniques (*24*) for classifying regional-continental sources of dust (*5, 8*) in terms of their mineral assemblages and sources. A recent study expresses different magnetic terms and units as partial susceptibilities thus allowing the contributions of different magnetic minerals in bulk road dust samples in Liverpool, U.K., to be modeled quantitatively with reasonable success (*25*). There is increasing evidence that magnetic properties may provide an important proxy for the organic components in respirable (PM_{10}) and larger urban particulates. Using frequency-dependent susceptibility (χ_{FD}) as a magnetic signature for submicron particles (*26*), it appears that much of the organic matter in Liverpool road dusts is derived from nonairborne eroded soil (*11*). In contrast, the magnetic susceptibility of respirable airborne particulates in Hamilton, Ontario, is strongly associated with mutagenicity (*7*) associated with certain keto- and thiapolycyclic aromatic hydrocarbons. The highest levels of mutagenicity and susceptibility were related to wind direction, low to moderate wind velocities, and enhanced levels of SO_2 and NO_2 but not to TSP loadings. Overall, significant evidence exists to suggest that magnetic measurements may be successfully used to determine areas influenced by specific pollution sources, to identify pollution pathways, to classify particulate sources, to analyze their Fe-mineralogy and grain-size, to model multiple source contributions in bulk samples, and to provide an effective proxy for organic and inorganic compounds and potential health risk.

The present paper reports results from a pilot investigation into the value and sensitivity of using magnetic techniques to define the types, sources, and transport mechanisms of

* Corresponding author phone: 0086-21-62233416; fax: 0086-21-62576217; e-mail: shuj@public4.sta.net.cn.
† East China Normal University.
‡ University of Liverpool.

10.1021/es9910964 CCC: $19.00
Published on Web 05/09/2000

TABLE 1. Location and Height from Ground of 11 Sampling Sites

district location	site no.	height from ground (m)	site location
Taopu Chemical industrial area (3 km^2) NW edge of the city center	1	7	about 200 m away from S edge of the Taopu chemical industrial area center
	2	6	in the W fringe of Taopu chemical industrial area
	4	7	in N edge of the above area
Residential quarter	3	16	about 2.5 km from W edge of the above area
	5	7	about 5.0 km S of above area; about 30 mW of elevated road under construction in city center
Baoshan iron and steel manufacturing and power generation complex N of the urban area: The six sampling sites span the W edge of the Baoshan district (424.6 km^2)	6	4	about 0.5−1.0 km SW of chemical plant and steelworks
	7	4	about 1.5−2.0 km NW of the steelworks and chemical plant, 2.0−3.0 km S of the iron and steel manufacturing complex, and 4 km NW of the sixth site
	8	18	about 1.0−2.0 km W of the iron and steel manufacturing complex and 5 km NW of site 7
Residential and lighter industry with three sites to the NW of the city between Baoshan and Taopu	9	4	sites 9−11, from N to S in this region, are used to contrast their TSP level at distance >5 km from Baoshan complex (sites 6, 7, 8)
	10	4	
	11	9	

[a] See also Figure 1.

TSPs in adjacent districts of Shanghai, China, over daily periods. These districts have high TSP loadings derived from a variety of airborne particulate sources, including iron and steel manufacturing, power generation, chemical industries, construction sites, motor vehicle emissions, and, under adverse weather conditions, wind erosion of local cultivated fields. It has been reported (*27*) that air pollution in Shanghai is of a compound type but characterized mainly by coal-smoke. The mean TSP concentration (264 μg m^{-3}) in the urban area in autumn 1996 was 23 μg m^{-3} higher than the annual mean value and 38 μg m^{-3} higher than the rural area in the same period (*27*). Information about the importance of different emission sources and their potential health effects on the local population are urgently required for designing, implementing, and monitoring pollution controls.

Sample Collection and Measurements. TSPs were collected at 11 sampling sites (Table 1) within and around the chemical industrial area (Taopu) and iron and steel and power generation complexes (Baoshan), located on the NW edge of the Shanghai city center and N of the Shanghai city area, respectively (Figure 1). Eleven medium volume TSP samplers, manufactured by Shanghai Hongyu Electronic Equipment Factory (*28*), were utilized to collect TSPs under meteorological conditions dominated by prevailing N and NW winds during the sampling period (November 5−11, 1998). These directions are prevailing early winter wind directions in Shanghai. Three PM_{10} samplers located at sites 2, 5, and 6 were also used to collect finer particulates during the same period for comparison with TSP samples. Near the 11th sampling site, an automatic weather station, made by Davis Instruments Corp. U.S.A., was used to supply meteorological data adjusted with records from the meteorological observatory.

Clean and preweighed glass fiber filters (diameter 100 mm) were kept in a desiccator for 24 h before loading into TSP sample holders. The sampling flow rate was set at 0.15 m^3 min^{-1}, and the total sampling time was 24 h per sample. The filters collect all grain-sizes in the range 0.1−100 μm. The filters with samples were kept in a desiccator for 24 h, and sample mass was calculated from weight difference. The sampling program gave 75 filters with TSP samples (site 5 was short of 2 days sampling) and 18 filters with PM_{10} samples (site 5 was short of 3 days sampling). Magnetic measurements were made on filter papers with samples folded into 10 mL plastic pots. The mean magnetic measurements of 10 clean filters for χ_{LF}, SIRM, and χ_{ARM} are 2.3753 ± 0.2401 (10^{-8} m^3 kg^{-1}), 7.0376 ± 0.3002 (10^{-5} Am^2 kg^{-1}), and 0.4614 ± 0.1107 (10^{-5} m^3 kg^{-1}), respectively. These positive magnetic values are explained by slight contamination during filter production but are insignificantly low compared with the dust samples. Magnetic susceptibility (χ 10^{-8} m^3 kg^{-1}) was measured using a dual-frequency (470 and 4700 Hz) Bartington Instruments MS2 susceptibility meter. Anhysteretic remanent magnetization (ARM 10^{-8}m^3 kg^{-1}) was induced in a steady field of 0.1 mT imposed on a peak AF field of 100 mT, and the remanence measured by a Molspin spinner magnetometer. Susceptibility of ARM (χ_{ARM} 10^{-8} m^3 kg^{-1}) is calculated by dividing the ARM by the size of the steady biasing field. Acquisition of isothermal remanent magnetization (IRM 10^{-5} Am^2 kg^{-1}) was made in fields of 20 mT, 30 mT, 1 T (SIRM) followed by demagnetization in fields of −20 mT, −50 mT, −100 mT, and −300 mT using a Molspin pulse magnetizer and spinner magnetometer. Measurements are expressed in both mass-specific and quotient bases in order to give quantitative and qualitative information about mineral types, domains, and grain-sizes. The following list describes the main magnetic parameters used in the study: χ_{LF} approximates to the total concentration of Fe-bearing minerals in the mineral assemblage but is controlled largely by the total ferrimagnetic concentration (*2*). $\chi_{FD} = \chi_{LF} - \chi_{HF}$ approximates to the total concentration of SP magnetite (*26*). SIRM approximates to the total remanence carrying mineral assemblage but is controlled largely by the stable single domain (SSD) magnetite concentration (*2*). ARM (χ_{ARM}) approximates to the concentration of SSD (and fine PSD) ferrimagnetic components (*29, 30*). SOFT remanence = (SIRM-IRM$_{-20mT}$)/2 approximates the concentration of low coercivity mineral phases, like magnetite, especially for grains in the MD domain range and possibly viscous SP/SSD range (*31*). HIRM = (SIRM−IRM$_{-300mT}$)/2 approximates the total concentration of high coercivity mineral phases such as canted antiferromagnetic hematite (*2*). SOFT % = 100*(SOFT/SIRM) approximates to the proportion of low coercivity mineral phases, like ferrimagnetic magnetite, relative to other remanence carrying minerals (*31*). HIRM % = 100*(HIRM/SIRM) approximates the proportion of high coercivity mineral phases, like canted antiferromagnetic hematite, relative to the total remanence carrying mineral assemblage (*2*). χ_{FD} % = 100*(χ_{LF}−χ_{HF})/χ_{LF}

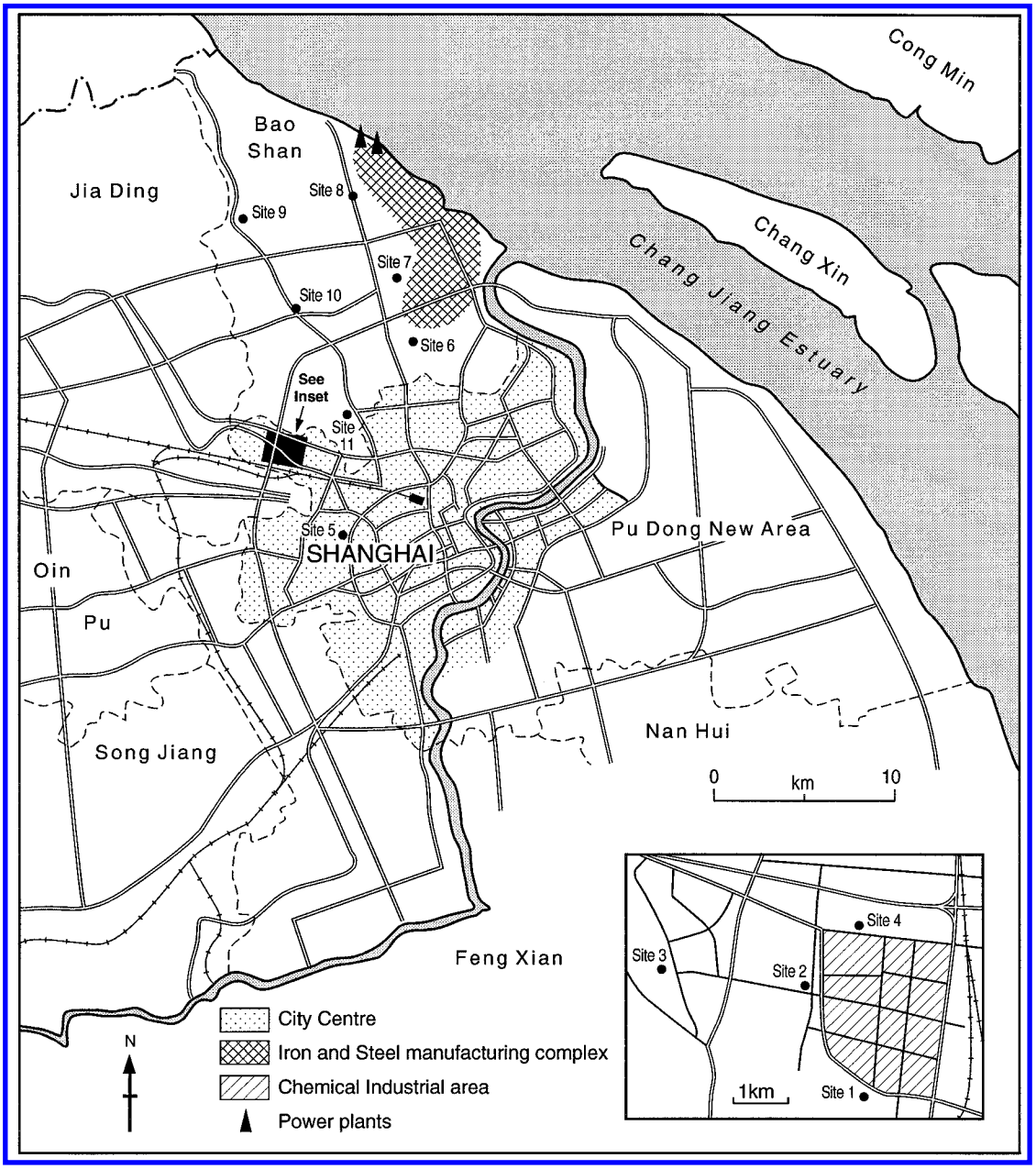

FIGURE 1. Shanghai, China. Location of sampling sites showing Baoshan iron and steel complex, power generation sites, and Taopu chemical industrial area (inset).

approximates the proportion of SP magnetite and may be interpreted semiquantitatively (*26*). SIRM/χ_{LF} is controlled by SSD magnetite grains and to a lesser extent the proportion of hematite (*2*). SIRM/χ_{ARM} is sensitive to the relative proportion of coarse SSD+PSD domains in domain sizes larger than SP (*29, 30*).

Results and Discussions

TSP Loadings and Daily Variations in Dust Magnetic Properties. Daily TSP concentrations generally vary between ~74 and 491 μg m^{-3} with a 1 day maximum of 1069 μg m^{-3} at site 5. Figure 2 shows daily TSP concentrations and magnetic measurements from two sites: site 6, close to the Baoshan industrial complex, and site 3, close to construction sites and residential quarters. At these sites and the others, there is a systematic pattern through the week of first decreasing and then increasing values for ferrimagnetic concentration parameters (χ_{LF}, SIRM, SOFT, and χ_{ARM}), with values tending to reach a minimum on Saturday and Sunday (days 4 and 5). Daily variations in quotient parameters, such as χ_{FD}%, SIRM/χ_{ARM}, and SIRM/χ_{LF} indicate magnetic domain sizes and mineralogy related to the changing site-specific importance of different dust sources. In general, TSP concentrations are negatively correlated with magnetic concentration parameters χ_{LF}, SIRM, χ_{ARM}, and HIRM (Figure 3). This shows that the quantitatively dominant sources of TSPs are characterized by weakly magnetic assemblages of minerals, often typified by very high SIRM/χ_{ARM} values >80 kAm^{-1} (Figure 2). The weak negative relationship between HIRM and TSP concentrations especially (Figure 3d) indicates that the major source of hematite minerals is probably less local and becomes progressively diluted at times of high dust deposition. These temporal variations suggest that city-wide TSP loadings and magnetic concentrations are strongly affected by daily fluctuations in industrial and commercial activities but that dust mineralogy and domain sizes at a site may reflect more the proximity to dust sources and meteorological conditions.

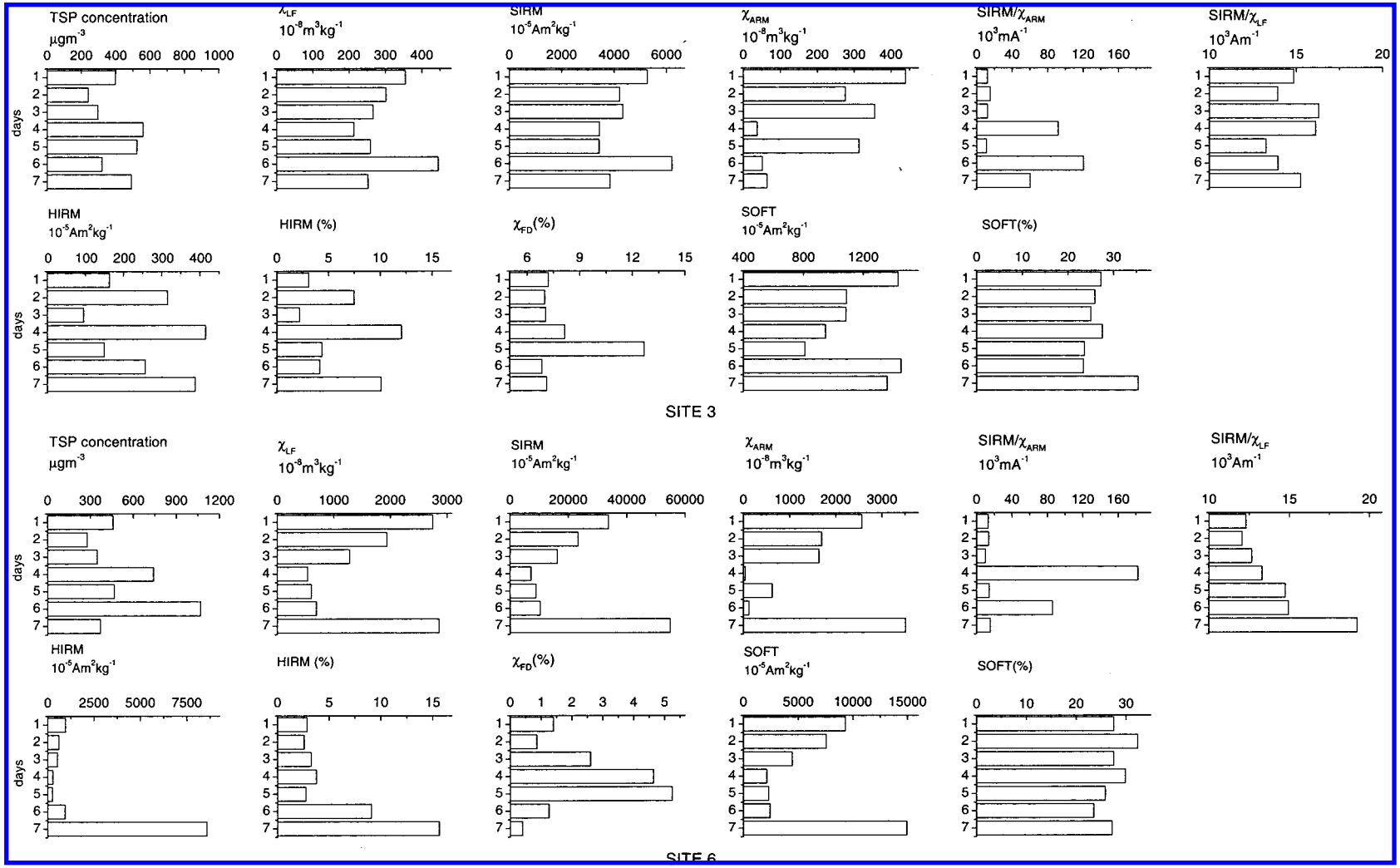

FIGURE 2. Magnetic measurements and TSP concentrations for sites 3 and 6. Days represented as 1: Wednesday-Thursday, 2: Thursday-Friday, 3: Friday-Saturday, 4: Saturday-Sunday, 5: Sunday-Monday, 6: Monday-Tuesday, 7: Tuesday-Wednesday.

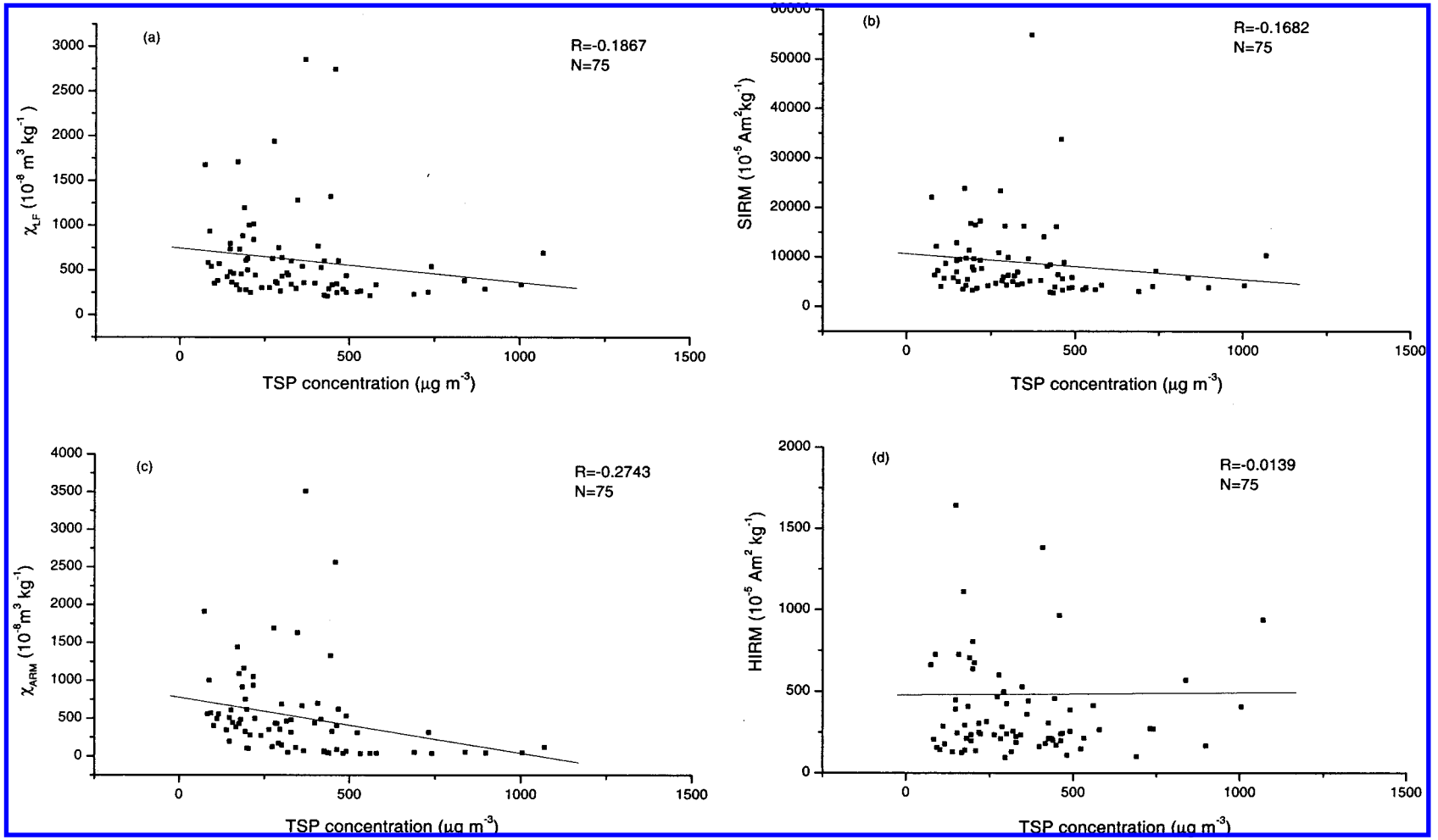

FIGURE 3. Correlation analysis between (a) TSP concentration and χ_{LF}; (b) TSP concentration and SIRM; (c) TSP concentration and χ_{ARM}; and (d) TSP concentration and HIRM. One point (site 6) excluded in (d) for clarity (TSP 370 μg m^{-3}; HIRM 8574.7 10^{-5} Am^2 kg^{-1}).

TABLE 2. Means and Standard Deviations for Magnetic Measurements of TSP Samples at 11 Sites

site	χ_{LF}[a]	χ_{FD}[b]	χ_{fd} %	SIRM[c]	χ_{ARM}[d]	SIRM/χ_{LF}[e]	HIRM[f]	HIRM %	SIRM/χ_{ARM}[g]	SOFT[h]	SOFT %
1	493.5 ± 167.5	35.8 ± 9.5	7.5 ± 1.7	6660.5 ± 2063.1	440.9 ± 322.9	13.6 ± 0.6	269.8 ± 118.8	4.1 ± 1.4	33.0 ± 30.94	1801.7 ± 480.7	28.0 ± 5.7
2	408.5 ± 145.2	28.4 ± 9.3	7.0 ± 0.8	5729.5 ± 2160.6	298.6 ± 228.4	14.0 ± 0.9	313.0 ± 222.4	5.4 ± 2.5	36.6 ± 30.7	1484.4 ± 555.6	26.0 ± 1.8
3	298.7 ± 72.4	23.4 ± 5.8	8.0 ± 1.9	4389.0 ± 944.4	219.4 ± 153.2	14.8 ± 1.1	254.43 ± 114.4	6.0 ± 3.5	46.1 ± 42.0	1168.0 ± 232.4	26.9 ± 3.8
4	523.7 ± 222.7	36.3 ± 13.9	7.1 ± 0.7	7294.8 ± 3069.6	403.0 ± 325.9	14.2 ± 2.7	406.7 ± 504.9	4.9 ± 3.5	36.2 ±30.2	1824.7 ± 835.3	24.9 ± 3.4
5	413.2 ± 112.1	22.8 ± 22.7	4.6 ± 3.4	5090.7 ± 1270.0	274.3 ± 188.6	12.4 ± 1.6	298.6 ± 164.2	6.1 ± 3.1	45.2 ±41.3	1463.4 ± 465.7	28.4 ± 3.7
6	1521.2 ± 925.6	23.6 ± 10.7	2.3 ± 1.8	22087.0 ± 15958.2	1454.0 ± 1196.3	14.2 ± 2.3	1731.8 ± 2806.0	5.7 ± 4.6	47.9 ±60.4	6162.1 ± 4421.6	27.7 ± 2.6
7	743.1 ± 304.5	36.5 ± 24.7	5.2 ± 2.7	11174.5 ± 4387.7	605.4 ± 427.4	15.1 ± 2.0	448.6 ± 389.4	4.1 ± 2.7	47.5 ± 50.5	2943.2 ± 1191.2	26.4 ± 3.1
8	1098.1 ± 454.2	66.0 ± 28.9	6.1 ± 0.9	15332.3 ± 6129.5	949.2 ± 612.8	14.2 ± 1.3	646.0 ± 254.3	4.4 ± 0.9	38.2 ± 50.7	4233.1 ± 1872.3	28.3 ± 4.7
9	410.3 ± 164.6	26.3 ± 5.1	7.0 ± 1.8	6669.8 ± 4396.8	347.9 ± 193.4	15.1 ± 3.5	252.3 ± 128.9	4.0 ± 0.9	37.8 ± 41.5	1673.0 ± 647.4	28.4 ± 6.8
10	441.1 ± 120.2	31.8 ± 8.3	7.5 ± 2.3	7006.2 ± 2476.8	379.6 ± 195.0	15.6 ± 2.7	418.4 ± 188.7	6.1 ± 1.7	31.1 ± 27.6	1770.2 ± 536.1	26.8 ± 6.9
11	327.8 ± 77.9	6.8 ± 8.3	6.8 ± 2.0	4977.8 ± 1430.8	314.6 ± 182.3	15.1 ± 1.5	216.2 ± 55.7	4.4 ± 1.1	30.0 ± 27.3	1346.6 ± 392.7	27.7 ± 6.7

[a] 10^{-8} m^3 kg^{-1}. [b] 10^{-8} m^3 kg^{-1}. [c] 10^{-5} Am^2 kg^{-1}. [d] $10^{-8}m^3$ kg^{-1}. [e] kAm^{-1}. [f] 10^{-5} Am^2 kg^{-1}. [g] kAm^{-1}. [h] 10^{-5} Am^2 kg^{-1}.

Spatial Variability in Magnetic Properties. Table 2 shows that mean magnetic properties of TSPs vary from site to site. In general terms, the highest mean and maximum magnetic concentrations (χ_{LF}, SIRM, $\chi_{ARM,}$ SOFT, and HIRM) are found at sites 6, 7, and 8, close to the Baoshan complex (Figure 1). These data are consistent with magnetic phases dominated by the coexistence of a low coercivity magnetite component, in varying domain ranges, and a high coercivity hematite component. Mean magnetic concentrations (χ_{LF}) at sites 9, 10, and 11, situated 5−10 km W of Baoshan (Figure 1), are 20−60% lower and similar to other sites close to the Taopu chemical industrial area (sites 1, 2, and 4) and residential quarters on the edge of city center (site 5). The lowest mean and maximum magnetic concentrations are found at site 3, another residential quarter lying a few kilometers W of Taopu (Figure 1).

Overall, the variability in quotient parameters is less than for concentration parameters. In particular, low variability in mean values for SOFT % (24−28%), SIRM/χ_{LF} (12−16 kA m^{-1}), and HIRM % (4−6%) across the sites (Table 2). Mean values for χ_{FD} % in the range 2.3−8.0 indicate significant but variable proportions of SP grains. SP grains not only are normally associated with secondary ferrimagnets formed in surface soil but may also be found in the finest-grained fly ash particles (*22*). Exceptions are samples from site 6 that have low χ_{FD} % values (mean 2.3%) and where high values for SOFT and SIRM/χ_{ARM} values may be interpreted as coarse-grained MD+PSD magnetite. Relatively high mean values of HIRM % (5.7%) at site 6 also suggest a significant proportion of high coercivity hematite.

The magnetic concentrations of daily PM_{10} samples (mass 0.003−0.036 g) were normally too weak to measure. Aggregating six daily samples (mass ∼0.1 g) for the magnetically strong site 6 gives repeatable magnetic measurements for χ_{LF}, SIRM, and χ_{ARM} of 269.0 10^{-8} m^3 kg^{-1}, 3454.0 10^{-5} Am^2 kg^{-1}, and 1130.7 10^{-8} m^3 kg^{-1}, respectively. These values are significantly lower than TSP samples from the same site (Table 2) as shown by ratios of magnetic values for PM_{10} to TSP for χ_{LF}, SIRM, and χ_{ARM} of 1:10, 1:10, and 1:2, respectively. Ratios of magnetic values for PM_{10} to TSPs at magnetically weaker sites (e.g. site 5 day 2) are 1:2.2, 1:2.0, and 1:0.5, respectively, showing the greater importance of magnetic phases in <10 μm fractions at sites further away from the heavy industrial complexes.

Sample Classification and Dust Sources. Thirteen concentration-dependent and concentration-independent parameters are employed as variables to define magnetic signatures for each TSP sample. Factor analysis was performed using the subprogram factor on the SPSS system with the minimum eigenvalue used to control the number of factors set as one and factor rotation block with varimax rotation specified. The results show that eigenvalues of SIRM/χ_{ARM}, HIRM, HIRM %, and SIRM/χ are greater than one, explaining 93% of total variance in the first four factors. From the rotated factor matrix, the extracted factor 1 is controlled by the concentration parameters SIRM, χ_{ARM}, SOFT, χ_{LF}, and HIRM (weighted factor $F_1 = 0.81$). Factor 2 mainly represents the influence of PSD+MD grains measured by SOFT % with SIRM/χ_{ARM} (weighted $F_2 = 0.57$). The results of hierarchical cluster analysis based on factors 1, 2, 3, and 4 gives a 4-fold classification (A−D) of the samples from 11 sampling sites: (A) area close to the Baoshan industrial complex (sites 6, 7, and 8); (B) areas about 8 km west of the Baoshan complex and on the southern fringe of the Taopu chemical industrial area (sites 1, 9, 10, and 11); (C) the northern and western fringes of Taopu (sites 2 and 4); and (D) suburban and inner city residential areas (sites 3 and 5).

The correlation coefficients between SIRM (magnetite) and HIRM (hematite) are reasonably strong ($r = 0.83$) for samples from sites in cluster A but decline with distance from Baoshan to a negative value ($r = -0.1$) in cluster D samples. This suggests that the contribution from the Baoshan complex at these sites is reduced and masked by other sources of dusts. Samples of particulate emissions from six new coal-fired power station stacks at Baoshan (NE of site 8) taken from above the electrostatic filters have been obtained. Values of χ_{LF}, SIRM, χ_{ARM}, and HIRM for these dusts are broadly of the same order or higher than the TSP samples from sites 6, 7, and 8 except for the quotients χ_{FD}% (0.8−3.8%) and SIRM/χ_{ARM} (6.2−11.9 10^3 Am^{1-}) which are considerably smaller than all TSPs but similar to PM_{10} samples. These results show that SSD grains, rather than larger PSD and MD grains, dominate the emissions from new power station stacks. The present difference between the domain size properties of TSPs and emission dusts from new stacks implies either efficient dispersal of finer particles away from the local environment or the overwhelming effect of older combustion technologies on TSP magnetic properties. If previously reported links between mutagenicity and magnetic concentration (*7*) are applicable here, the present data suggest a significant health risk for populations in at least the N and NW districts of Shanghai. Analyses of organic and inorganic

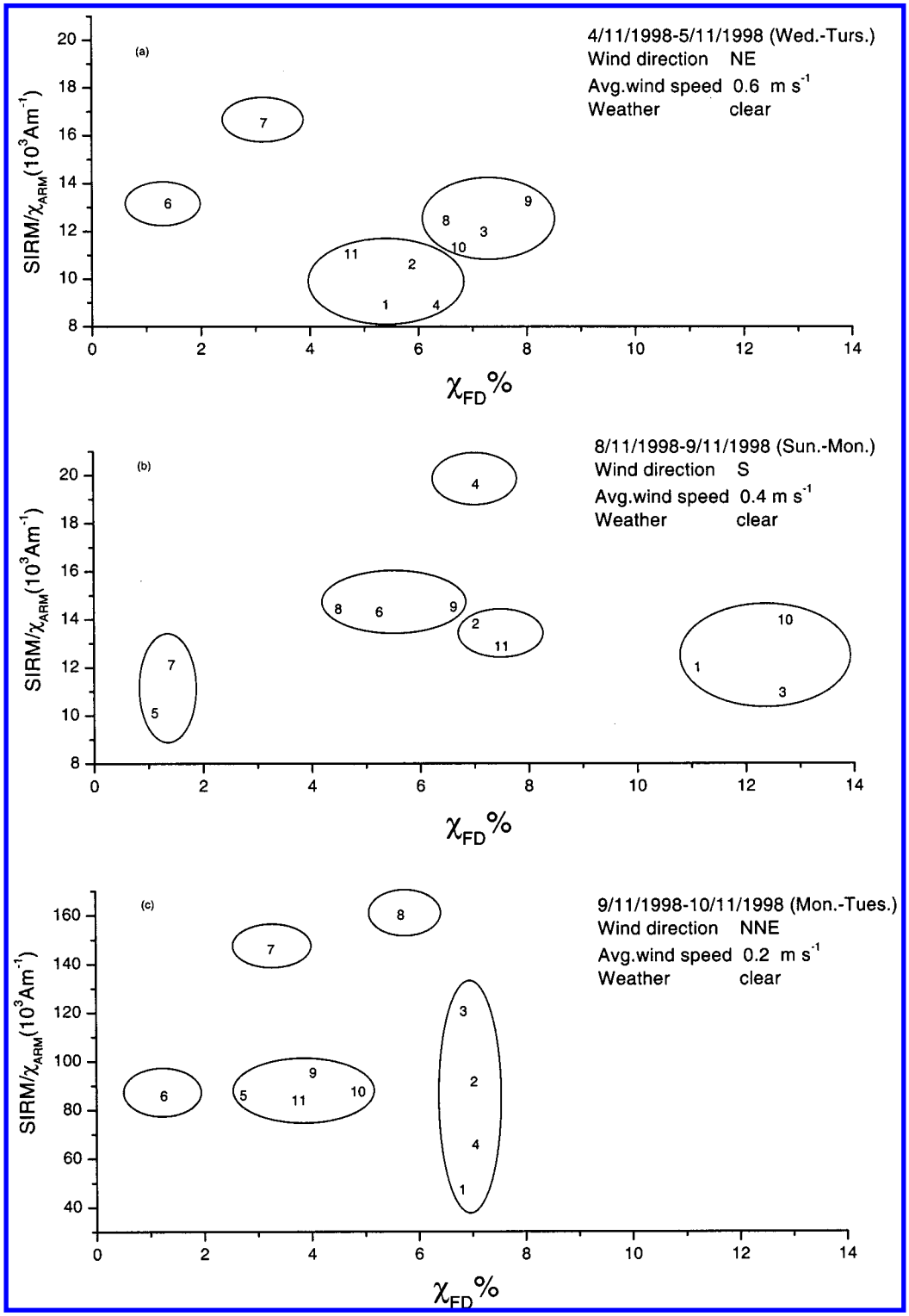

FIGURE 4. SIRM/χ_{ARM} verus χ_{FD} % plotted for TSPs sampled at 11 sites (numbered 1−11) across Shanghai for three 24 h periods: (a) 4/11/98−5/11/98; (b) 8/11/98−9/11/98; and (c) 9/11/98−10/11/98. Data for site 5 (a) not available. Note change of axis scale in (c).

compounds contained in the samples and magnetic measurements of other "pure" pollution source materials are ongoing.

Wind Controls on Magnetic Variability. The wind velocities were relatively weak (0.2−0.6 m s^{-1}) during the sampling period and northerly except for a southerly wind on day 5. It is therefore likely that long-distance transported particles were less significant than local pollution sources over the period. Daily changes in mineral assemblages and sources may be gauged by using a semiquantitative mixing model (*32*) based on χ_{FD}% and SIRM/χ_{ARM} values to estimate the proportions of domain sizes in daily samples over 7 days at each site. At all sites the most frequent daily assemblage (Table 3) comprises SP (10−50%) and MD+PSD (50−90%). Sites 6 and 7 close to the iron and steel complex and site 5 close to the urban center also had days dominated by lower

TABLE 3. Number of Days at Each Site with Different Proportions of SP and MD+PSD Grain Assemblages Estimated from Semiquantitative Mixing Model

		site										
		1	2	3	4	5[a]	6	7	8	9	10	11
SP	10%					1	4	1				
MD+PSD	90%											
SP	10−50%	5	6	5	6	3	3	4	7	5	6	6
MD+PSD	90−50%											
SP	50−75%	1	1	1	1			2		2		1
MD+PSD	50−25%											
SP	75−100%	1		1		1					1	
MD+PSD	≤25%											

[a] Site 5 was short of 2 days sampling.

proportions of SP grains, while all sites except for 5, 6, and 8 had days where the SP component was greater or even dominated.

Wind direction has a significant effect on daily magnetic domain size and mineralogies as shown by the semiquantitative interpretation of SIRM/χ_{ARM} versus χ_{FD} % plots for the sample set over 3 different days (Figure 4). For example, samples taken 4/11/98−5/11/98 were affected by a dominant NNE wind (Figure 4a) and show relatively high values of SIRM/χ_{ARM} and low values of χ_{FD} %, at sites 6 and 7 located S of Baoshan and medium high values of χ_{FD} % at other sites. Samples at sites 6 and 7 are interpreted as containing SP and MD+PSD grains in the proportions ∼10%:∼90%, and 10−50%:90−50%, respectively, while other sites show higher proportions of SP grains and lower proportions of MD+PSD grains. A shift to a S wind during the period 8/11−9/11/98 (Figure 4b) is linked to very low values of χ_{FD} % and consequently insignificant proportions of SP grains at sites 5 and 7, close to the construction site of an elevated road around the city center and downwind of Baoshan, but χ_{FD} % values >10% at sites 1, 3, and 10 indicative of a significant upwind source of SP grains. These three sites are close to the rural fringe or building and road construction sites, and wind-blown soil with secondary ferrimagnetic minerals seems the most probable dust source. It appears that the city-wide impact of the Baoshan complex seems to be substantially reduced during a southerly airflow, and the domain assemblage becomes considerably finer (SP 10−50%). The return of a low velocity NNE wind the following day (9/11−10/11/98) was associated again with high concentrations of coarser domain magnetic minerals at all sites (Figure 4c), particularly sites 6 and 7 close to Baoshan. Values for SIRM/χ_{ARM} significantly increased in all samples reaching a maximum for this sampling period, possibly indicating a strong coarsening of grain sizes at all sites linked to short distance transport from local sources, such as vehicle emissions (*18*, *33*). Magnetic properties are thus sufficiently sensitive to monitor shifts in particulate sources caused by daily changes in wind conditions. An expanded network of sampling sites across the city would provide source data for daily monitoring of point sources, regional sources, and the testing of pollution dispersion models.

Acknowledgments

We gratefully acknowledge financial support by the National Natural Science Foundation of China (Project Approval No. 49671069) and the University of Liverpool. Mr. Bob Jude and Mr. Nu Yuan provided valuable help with magnetic measurements. Mr. Baogen He, Mr. Liantang Den, Mr. Tianhan Jiang, and Mr. Xiaomin Yang provided the particulate samples. Drs. S. J. Sangode, J. Reinders, Yuquan Hu, Weiguo Zhang, Ming Liu, and Yu Xu and two anonymous reviewers provided useful comments on the work. We thank Mrs. Sandra Mather for the cartography.

Literature Cited

(1) Elson, D. M. *Atmospheric Pollution: A Global Problem*; Blackwell Oxford: U.K., 1995; Chapter 1.
(2) Thompson, R.; Oldfield, F. *Environmental Magnetism*; Allen and Unwin: London, 1986; Chapter 11.
(3) Petrovsky, E.; Ellwood, B. B. In *Quaternary Climate, Environment and Magnetism*; Maher, B. A., Thompson, R., Eds.; Cambridge University Press: Cambridge, 1999; Chapter 8.
(4) Chester, R.; Sharples, E. J.; Sanders, G.; Oldfield, F.; Saydam, A. G. *Water, Air Soil Pollut.* **1984**, *23*, 25−35.
(5) Hunt, A. *Phys. Earth Planet Int.* **1986**, *42*, 10−21.
(6) Hunt, A.; Jones, J.; Oldfield, F. *Sci. Total Environ.* **1984**, *33*, 129−139.
(7) Morris, W. A.; Versteeg, J. K.; Bryant, D. W.; Legzdins, A. E.; McCarry, B. E.; Marvin, C. H. *Atmos. Environ.* **1995**, *29*, 3441−3450.
(8) Oldfield, F.; Hunt, A.; Jones, M. D. H.; Chester, R.; Dearing, J. A.; Olsson, L.; Prospero, J. M. *Nature* **1985,** *317*, 516−518.
(9) Beckwith, P. R.; Ellis, J. B.; Revitt, D. M.; Oldfield, F. *Phys. Earth Plant Int.* **1986,** *42*, 67−75.
(10) Xie, S.; Dearing, J. A.; Bloemendal, J.; Boyle, J. F. *Sci. Total Environ.* **1999**, *241*, 205−214.
(11) Xie, S.; Dearing , J.A.; Bloemendal, J. *Atmos. Environ.* **2000**, *34*, 269−275.
(12) Dearing, J. A.; Lees, J. A.; White, C. *Geoderma* **1995**, *68*, 309−319.
(13) Hay, K. L.; Dearing, J. A.; Baban, S. M. J.; Loveland, P. J. *Phys. Chem. Earth* **1997**, *22*, 207−210.
(14) Strzyszcs, Z.; Magiera, T.; Heller, F. *Studia Geoph. Geod.* **1996**, *40*, 276−286.
(15) Schiavon, N.; Zhou, L. *Environ. Sci. Technol.* **1996**, *30*, 3624−3629.
(16) Flanders, P. J. *J. App. Phys.* **1994**, *75*, 5931−5936.
(17) Flanders, P. J. *Environ. Sci. Technol.* **1999**, *33*, 528−532.
(18) Matzka, J.; Maher, B. A. *Atmos. Environ.* **1999**, *33*, 4565−4569.
(19) Oldfield, F.; Thompson, R.; Barber, K. E. *Science* **1978**, *199*, 679−680.
(20) Oldfield, F.; Richardson, N. *Philos. Trans. R. Soc. London B* **1990**, *327*, 325−330.
(21) Querol, X.; Parés, J. M.; Plana, F.; Fernández-Turiel, J.. López-Soler, A. *Environ. Geochem. Health* **1993**, *15*, 9−18.
(22) Dekkers, M. J.; Pietersen, H. S. *Mater. Res. Soc. Symp. Proc.* **1992**, *245*, 37−47.
(23) Xie, S.; Dearing, J. A. *Environ. Sci. Technol.* **1999**, *33*, 41−40.
(24) Yu, L.; Oldfield, F. *Quat. Res.* **1989**, *32*, 168−181.
(25) Xie, S.; Dearing, J. A. Bloemendal, J. *Geophys. J. Int.* **1999**, *138*, 851−856.
(26) Dearing, J. A.; Dann, R. J. L.; Hay, K.; Lees, J. A.; Loveland, P. J.; Maher, B. A.; O'Grady, K. *Geophys. J. Int.* **1996**, *124*, 228−240.
(27) *Shanghai Environmental Bulletin-1996*; Shanghai Municipal Environmental Protection Bureau: June 1997.
(28) Ji, X.i; Jiang, D.; Fei, S.; Yuan, H.; He, P.;, Ye, B.; Lei, Z.; Feng, C. *Environ. Sci. Technol.* **1993**, *27*, 1735−1741.
(29) King. J.; Banerjee, S. K.; Marvin, J.; Özdemir, Ö. *Earth Plant Int.* **1982**, *130*, 727−736.
(30) Maher, B. A. *Geophys. J.* **1988**, *94*, 83−96.
(31) Thompson. R. *Phys. Earth Plant Int.* **1986**, *42*, 113−127.
(32) Dearing, J. A.; Bird, P. M.; Dann, R. J. L.; Benjamin, S. F. *Geophys. J. Int.* **1997**, *130*, 727−736.
(33) Hoffmann, V.; Knab, M.; Appel, E. J. *Geochem. Explor.* **1999**, *99*, 313−326.

Received for review September 23, 1999. Revised manuscript received January 27, 2000. Accepted February 29, 2000.

ES9910964